

Imaging vibrations inside acoustofluidic devices

SmarAct GmbH

INTRODUCTION

Microfluidic platforms comprise channel networks allowing the manipulation of fluids. Typically, they are used to detect and separate suspended particles such as viruses or cells. The sorting mechanism that is used in these lab-on-a-chip devices differ: while some make use of functionalized surfaces, others employ lasers or ultrasound, see Figure 1.

Ultrasonic standing waves permit the formation of controlled pressure fields which allow trapping of particles in up to 3 dimensions. Thus, adding acoustics to microfluidics increases the performance while remaining simple to produce and use. Ultrasounds are generated by a small piezo transducer that is attached to the capillary network. The frequency and amplitude of the vibrations are the key factors for trapping a desired group of particles.

Characterizing the performance of such devices using standard interferometry or vibrometry remain however tedious as they are mostly made of glass or silicon. It has also been shown that the vibrations transmitted to the different surfaces of the channel can greatly vary. Thus, without an instrument capable of selecting the surface on which the measurements are carried out, it is impossible to accurately evaluate the device. Here, we show how SmarAct's **PICOSCALE Vibrometer** can be used to easily overcome this limitation.

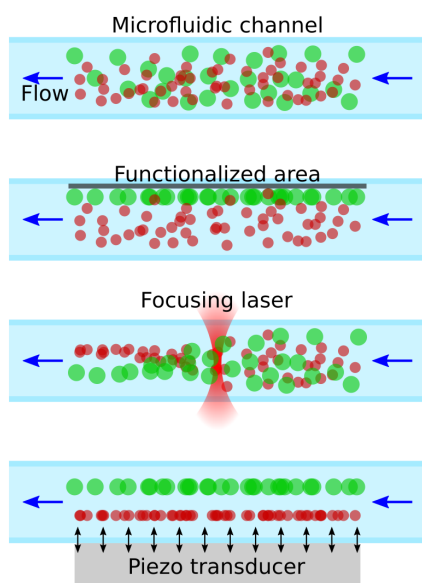


Figure 1. Sorting particles within microfluidic devices. It is possible to sort particles using different mechanisms: surface functionalization or transduced-vibrations are two examples.

RESULTS

Because the **PICOSCALE Vibrometer** uses confocal optics, it is possible to select any surface for further investigation. Figure 2 shows a focusing curve measured on an empty microfluidic channel. 4 peaks, labeled *a* to *d*, are clearly visible and correspond to the various interfaces of the glass channel. It should be noted that by virtue of Snell's law, the refractive index of the material results in a focus shift of the measurement laser. When passing through glass, the peaks will therefore appear closer together by a factor of ≈ 1.5 (refractive index of glass at 1550 nm). Thus, the measured thickness of 145 μm in Figure 2 translates into a real thickness of 218 μm , which agrees with the manufacturer's specification. The internal height of the (air-filled) microfluidic channel is 1011 μm .

Next, we measured the vibrational response of both surface *b* and *c*, considering that their behavior directly manipulates the fluid. To do so, the piezo transducer was excited by a 100 ms linear chirp from 500 kHz to 1 MHz generated by the **PICOSCALE Vibrometer**. Figure 3a shows multiple discrepancies between both curves. For instance, surface *b* shows a clear resonance at 630 kHz, at surface *c* this peak is completely shadowed by a peak at 616 kHz.

Because the measurements were performed at a single point it is not possible to attribute a specific vibrational mode to any of the resonance peaks. Even if both surfaces share similar resonances, such as at 820 kHz, it does not necessarily imply that they behave

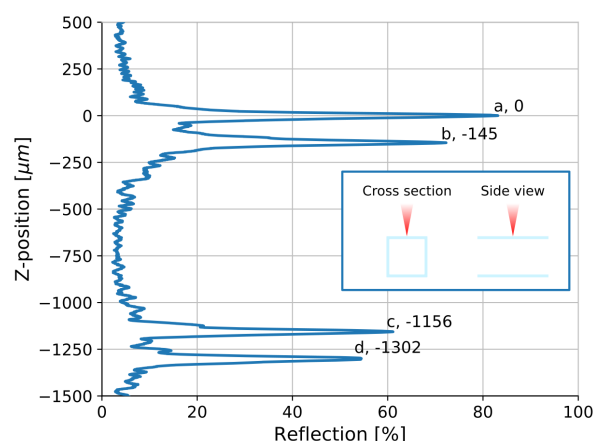
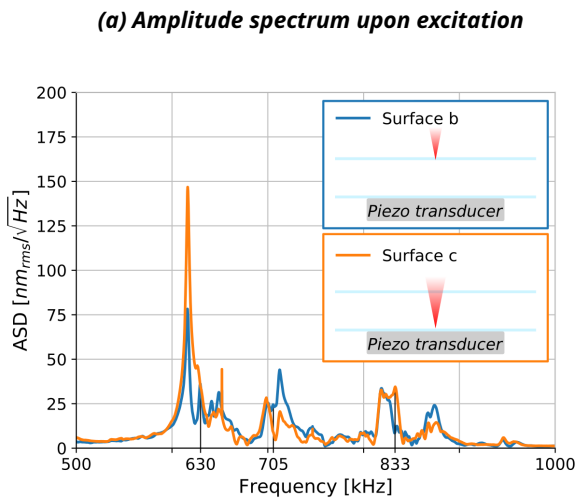


Figure 2. Focusing curve recorded on an empty microfluidic channel. By moving the focused measurement laser beam of the confocal microscope down while recording the reflection signal, the different surfaces of the channel are easily distinguished.



(b) Modal analysis at 820 kHz

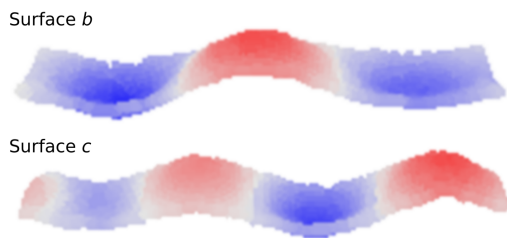
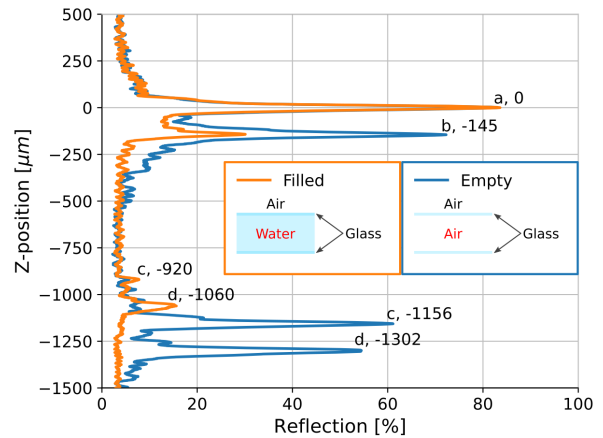


Figure 3. a) Thanks to the confocal optics of the *PICOSCALE Vibrometer* vibrations at both surface *b* and *c* were measured. The surfaces respond differently. The amplitude spectral density (ASD) is normalized with respect to the excitation signal. **b)** Surface *b* shows a lower order bending mode than surface *c*.

the same way. To emphasize this point, modal analysis at 820 kHz has been carried out at each of the surfaces. Surprisingly, Figure 3b reveals a higher order bending mode for surface *c* than for surface *b*.

So far, the microfluidic device was tested empty and having a fluid passing through the channel will inevitably affect the vibrational response. To assess this, the channel was filled with water and a focusing curve was recorded. Figure 4a shows that the position of the surfaces *c* and *d* has been shifted so that the measured internal height of the microfluidic channel is reduced by a factor of 1.3 (refractive index of water at 1550 nm) to 775 μm . Additionally, the amount of reflected light by both surfaces is drastically reduced. This comes from the fact that the water itself absorbs infrared light but also because the difference in refractive index between water and glass is much smaller than that between air and glass, which makes the interface more difficult to detect. In the water-filled channel the local vibrations at surface *b* were measured again, see Figure 4b. Some of the original peaks appear downshifted by approximately 6 kHz which together with Hooke's law, confirm that some mass, here the fluid, has been added to the system.

(a) Focusing on an empty and water-filled channel



(b) Amplitude spectra of empty vs. water-filled channel

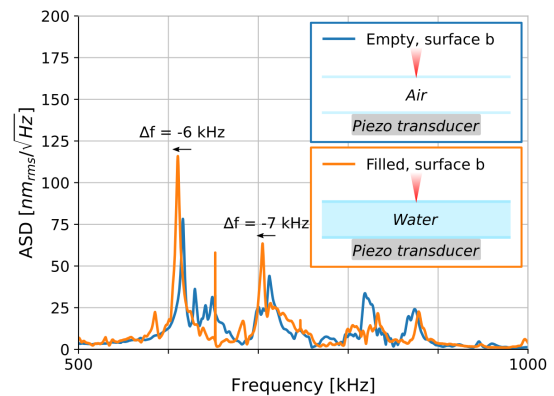


Figure 4. a) Because of the refractive index of the water, the peaks appear at a different positions and the amount of reflected light is reduced. **b)** The addition of a fluid inside the channel adds some mass to the system which alters the vibrational response. The amplitude spectral density (ASD) is normalized with respect to the excitation signal.

CONCLUSION

Confocal vibrometry with infrared light enables the imaging of internal surfaces of microfluidic flow cells. The high bandwidth of the *PICOSCALE Vibrometer* allows to visualize vibrations at up to 2.5 MHz, paving the way to an in-depth understanding of the functioning of acoustofluidic devices.

ACKNOWLEDGMENTS

We thank the Mechanics and Experimental Dynamics group at the ETH Zurich for their support with this application note.

Sales partner / Contacts

Germany

SmarAct GmbH

Schuette-Lanz-Strasse 9
26135 Oldenburg
Germany

T: +49 441 - 800 879 0
Email: info-de@smaract.com
www.smaract.com

France

SmarAct GmbH

Schuette-Lanz-Strasse 9
26135 Oldenburg
Germany

T: +49 441 - 800 879 956
Email: info-fr@smaract.com
www.smaract.com

USA

SmarAct Inc.

2140 Shattuck Ave. Suite 302
Berkeley, CA 94704
United States of America

T: +1 415 - 766 9006
Email: info-us@smaract.com
www.smaract.com

China

Dynasense Photonics

6 Taiping Street
Xi Cheng District,
Beijing, China

T: +86 10 - 835 038 53
Email: info@dyna-sense.com
www.dyna-sense.com

Natsu Precision Tech

Room 515, Floor 5, Building 7,
No.18 East Qinghe Anning
Zhuang Road,
Haidian District
Beijing, China

T: +86 18 - 616 715 058
Email: chenye@nano-stage.com
www.nano-stage.com

Shanghai Kingway Optech Co.Ltd

Room 1212, T1 Building
Zhonggeng Global Creative Center
Lane 166, Yuhong Road
Minhang District
Shanghai, China

Tel: +86 21 - 548 469 66
Email: sales@kingway-optech.com
www.kingway-optech.com

Japan

Physix Technology Inc.

Ichikawa-Business-Plaza
4-2-5 Minami-yawata,
Ichikawa-shi
272-0023 Chiba
Japan

T/F: +81 47 - 370 86 00
Email: info-jp@smaract.com
www.physix-tech.com

South Korea

SEUM Tronics

1109, 1, Gasan digital 1-ro
Geumcheon-gu
Seoul, 08594,
Korea

T: +82 2 - 868 10 02
Email: info-kr@smaract.com
www.seumtronics.com

Israel

Trico Israel Ltd.

P.O.Box 6172
46150 Herzeliya
Israel

T: +972 9 - 950 60 74
Email: info-il@smaract.com
www.trico.co.il